On the Financial Consequences of Simplified Battery Sizing Models without Considering Operational Details

Nam Trong Dinh^a, Sahand Karimi-Arpanahi^a, S. Ali Pourmousavi^a, Mingyu Guo^a, Julian Lemos-Vinasco^b, Jon A. R. Liisberg^b

 $^aThe\ University\ of\ Adelaide,\ Australia$ $^bWatts\ A/S,\ Denmark$

Abstract

Existing battery sizing methods tend to oversimplify battery operation within their sizing frameworks by ignoring several practical aspects of operation. Such assumptions may lead to suboptimal battery capacity, resulting in significant financial losses in battery projects. In this study, we compared the most common existing battery sizing methods in the literature with a battery sizing model that incorporates more realistic battery operation, specifically using receding horizon operation, also known as model predictive control. This approach continuously updates battery decisions based on new data and forecasts, ensuring realistic operation over the sizing period. In our comprehensive simulation studies, we quantified the financial losses caused by the suboptimal capacities obtained by these models for a realistic case study related to community battery storage (CBS). We developed a case study by constructing a mathematical framework for CBS and local end users. Our analysis indicates that conventional sizing strategies can cause financial losses as much as 22% in a simulation study with 84-day out-of-sample data including 120 end users in real wholesale market scenarios in New South Wales, Australia.

Keywords: Battery sizing, community battery, peak demand, receding horizon operation, price-responsive consumers

Nomenclature

Indices, Sets and Vectors

n/N Index/Set of end users

j/J Index/Set of receding horizons

h/H Index/Set of time intervals in a receding horizon

 H^{RB} Set of time intervals in a rebound horizon

Parameters

 β End-user price elasticity

 \hat{x} End-user originally expected consumption (kWh)

 $\overline{x}/\underline{x}$ Upper/lower bounds of end-user energy consumption (kWh)

 Δx End-user total consumption deviation (kWh)

 κ End-user short-term discounting degree

au End-user long-term discounting degree

 C^{init} End-user initial solar credits (kWh)

 Δh Length of time interval (h)

 E^{cap} CBS capacity (kWh)

SoC/SoC Upper/lower bounds of CBS state-of-charge (%)

 $\lambda^{\rm bat}$ CBS annualised per-unit cost (\$/kWh·year)

 Γ CBS round-trip efficiency (%)

 E^{init} CBS initial state-of-charge (kWh)

 λ^{ThP} CBS throughput cost (\$/kWh)

G Available rooftop solar energy (kWh)

 λ^{PD} Wholesale market pre-dispatch price (\$/kWh)

 $\lambda^{\rm RT}$ Real-time wholesale market price (\$/kWh)

 $\lambda^{\rm ImP}/\lambda^{\rm ExP}\,$ End-user import/export energy charge (\$/kWh)

 $\lambda^{\rm g}$ CBS operator grid usage charge (\$/kWh)

 λ^{peak} Peak demand incentive (\$/kW·year)

 Υ^{user} Users aggregated peak demand (kW)

 T^{c} CBS duration (h)

Variables

x End-user consumption (kWh)

 x^+/x^- End-user positive/negative net demand (kWh)

 x^{g} End-user billable consumption from utility grid (kWh)

 G^{u} Utilised rooftop solar energy (kWh)

 δ End-user solar credit offset (kWh)

D End-user (dis)comfort function

C End-user cumulative solar credits (kWh)

P CBS dispatch power (kW)

 $P^{\rm ch}/P^{\rm dc}$ CBS charging/discharging power (kW)

E CBS state of energy (kWh)

 ϑ^+/ϑ^- Community positive/negative net demand (kWh)

 ϑ^{g} Imported energy from the utility grid for charging CBS (kWh)

Υ^{local} Community peak demand (kW)

1. Introduction

Community battery storage (CBS) has been recognised as a desirable solution for behind-the-meter (BTM) generation and demand management both in practice [1, 2, 3], and in the literature [4, 5, 6]. In Australia, the trial of multiple CBS projects has led many distribution network service providers (DNSPs) to design new network tariffs specifically for CBS and end users within the neighbourhood [7, 8]. These tariffs generally incentivise the local use of the system (LUoS) for CBS located in low-voltage (LV) networks. As these schemes are designed to attract profit-making entities in the near future [9, 8], it is crucial to accurately size CBS to maximise the profits of CBS owners.

In recent years, many research studies have been published on battery storage sizing [10]. However, the existing sizing models in the literature do not consider the practical aspects of battery operation. In these studies, a common approach is to assume a perfect prediction of power system parameters, e.g., electricity prices [11], and power consumption [12], to solve the planning problem over the entire sizing horizon, e.g., one year [13]. These models guarantee a fast solution and can be scaled up for longer planning horizons, e.g., ten years. However, in practice, perfect knowledge of the future, even a couple of hours ahead, is impossible due to inherent uncertainties; hence, the battery operator's decisions can only be made under imperfect forecasts over a limited horizon, e.g., 24 hours ahead. To address this, many battery sizing studies optimise system capacity under a perfect foresight scenario and then apply a derating factor based on empirical percentage of perfect foresight [14]. Others introduce uncertainty by applying randomly generated noise to the perfect foresight values over the entire sizing horizon and solve the problem as a one-shot optimisation [15, 16]. Although convenient, this approach can be misleading in fast-evolving electricity markets, particularly those with high renewable penetration. In such environments, the predictability and uncertainty of key optimisation inputs, such as electricity prices, can degrade rapidly over time due to market volatility and changes in policy.

As an alternative to static derating methods, Baker et al. [17] proposed a battery storage sizing approach based on receding horizon operation (RHO), also known as model predictive control (MPC). In this operational concept, the operator solves battery optimisation by predicting the parameters of the power system for a specified lookahead horizon. The operator then only commits to the optimised solutions in the first interval of each receding horizon, while the remaining intervals ensure that the optimisation is not myopic. The optimisation problem must then be solved consecutively for the next receding horizons as new forecast data become available, a process that can be time- and resourceintensive. To address this issue, the authors in [17, 18, 19] coupled all receding horizons together, rather than solving the optimisation problem sequentially, to solve them simultaneously as a single optimisation problem. However, this coupling approach can negatively affect the optimal solutions because one horizon can be strongly influenced by many subsequent shifted horizons, which is not the way a battery unit operates in practice. This misalignment may eventually result in suboptimal decisions about battery capacity. In general, while previous research has introduced the perfect scenario or MPC-based battery sizing methods, these approaches have not been rigorously benchmarked against a globally optimal solution. Consequently, the true financial cost of using simplified sizing techniques remains largely unknown in the literature, particularly in the context of CBS projects, which are rapidly deployed in Australia. It should be noted that other operational factors can also influence battery performance and sizing outcomes, such as variations in efficiency and available capacity [20], caused by many factors, including real-time temperature and long-term degradation [21, 22]. Although these detailed aging models are highly relevant for long-term asset planning and performance evaluation, they fall outside the scope of this study. Here, we focus specifically on the role of operational control assumptions during the sizing phase, with particular emphasis on the impact of RHO under imperfect forecasts.

In this context, the first contribution of this paper is the quantification of financial losses resulting from the implementation of suboptimal battery capacities due to simplified battery sizing methods. This is achieved by developing a mixed-integer linear programming (MILP) model and solving the battery operation problem using an RHO approach. The second contribution is the reformulation of the approach in [17] for CBS sizing. To ensure accurate quantification, an exhaustive search is used to determine the global optimal battery capacity for comparison with suboptimal solutions, allowing a comprehensive evaluation of the inaccuracies of current sizing models.

2. Local market modelling with CBS

Current CBS trials in Australia allow solar end users (prosumers) within a local neighbourhood to virtually store their excess solar photovoltaic (PV) power in CBS in exchange for solar credits [1, 2, 3]. At night, prosumers can use solar credit to offset their consumption. In addition, the CBS operator collaborates with an existing electricity retailer to propose a time-of-use tariff structure with a high tariff during peak demand hours to promote a price-based demand response. The high peak demand tariff directs local prosumers to use their solar credit to offset consumption during those hours, typically in the early evening. Thus, the CBS operator automatically offsets prosumers' usage in the first instance of peak-demand hours. Nonetheless, some retailers allow residential customers to pay for electricity at spot prices obtained in the Australian National Electricity Market (NEM), together with the network tariffs set by DNSPs [23]. The NEM operates as a 5-minute real-time (RT) market managed by the Australian Energy Market Operator (AEMO). However, due to limitations in residential metering, these customers are still billed based on 30-minute intervals, with prices averaged over six consecutive 5-minute intervals. This tariff structure enables prosumers to decide when to offset their consumption depending on RT prices and their available solar credits. The fluctuation of RT prices also encourages prosumers to practice demand response to minimise their electricity bills [24]. Therefore, in this paper, we adopt the price-responsive model from [6, 25] to model end-user behaviour under fluctuations in RT prices, while also considering realistic network usage charges from DNSPs when storing electricity in CBS and consuming energy from CBS.

To accurately model the problem in an imperfect scenario, we solve optimisation models using predispatch (PD) prices provided by AEMO [26]. PD prices are forward-looking market signals with 30-minute intervals generated by AEMO several hours ahead and updated every 30 minutes. These prices are derived from a security-constrained linear optimal power flow model that considers the AEMO demand forecast and bids from market participants [27]. As demand forecasts change and participants rebid throughout the day, the PD prices fluctuate. Therefore, we use PD prices as electricity price forecasts in each receding horizon, which is also the case for many electricity retailers [23].

2.1. End-user Model

Although PD prices provide rolling electricity price predictions, there is still no dataset available for continuously updated forecasts of residential price-responsive consumption. To this end, we solve the end-user optimisation problem in an RHO framework to obtain the dynamic consumption behaviour for each receding horizon. The end-user RHO model is shown in Fig. 1.

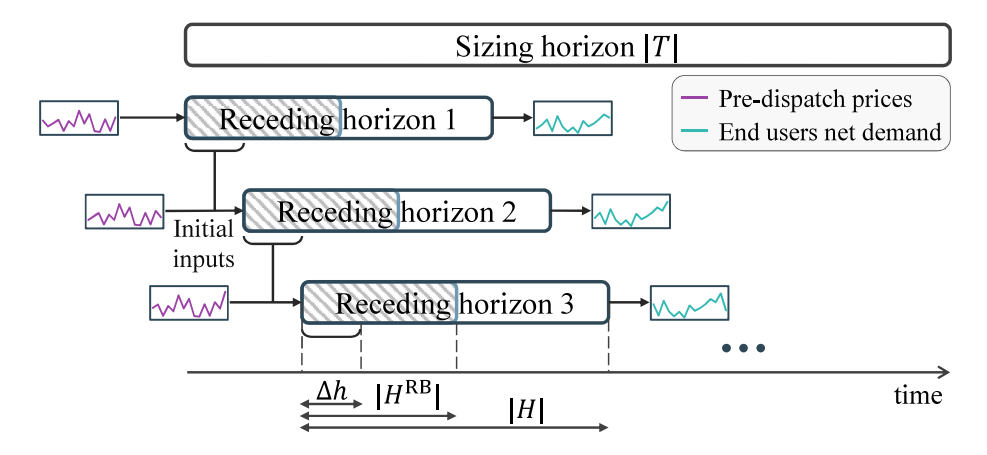


Figure 1: A flowchart showing end users RHO framework

We denote the set of end users by $N = \{1, 2, ..., |N|\}$. In RHO, the op-

timisation is solved each time on a receding horizon that includes the set of time intervals $H = \{1, 2, \cdots, |H|\}$, where |H| is the number of intervals in each horizon, and the optimisation recedes one interval each time. Overall, the optimisation problem is solved |J| times for all receding horizons, denoted by $j \in J = \{1, 2, \cdots, |J|\}$, where |J| represents the length of the battery sizing horizon. For each receding horizon j, the end-user optimisation can be formulated as follows:

$$\min_{\mathbf{\Psi}_{\mathbf{n},\mathbf{j}}} O_{n,j}^{\text{user}} = \sum_{h \in H} \left[\lambda_{j,h}^{\text{PD}} x_{n,j,h}^{\text{g}} + \lambda_{j,h}^{\text{ExP}} x_{n,j,h}^{-} + \lambda_{j,h}^{\text{ImP}} x_{n,j,h}^{+} + \frac{1 + \tau_n \cdot h \cdot \kappa_n}{1 + h \cdot \kappa_n} D(x_{n,j,h}) \right] \quad \forall n \in \mathbb{N}, \tag{1a}$$

where

$$D(x_{n,j,h}) = -\lambda_{\max,j}^{PD} \left(1 + \frac{x_{n,j,h} - \hat{x}_{n,j,h}}{2\beta_{n,j,h} \hat{x}_{n,j,h}} \right) (x_{n,j,h} - \hat{x}_{n,j,h})$$
(1b)

s.t.

$$\sum_{h \in H^{\text{RB}}} x_{n,j,h} = \sum_{h \in H^{\text{RB}}} \hat{x}_{n,j,h} + \Delta x_{n,j} \quad \forall n \in N,$$
(1c)

$$\underline{x}_{n,j,h} \le x_{n,j,h} \le \overline{x}_{n,j,h} \quad \forall n \in N, \ \forall h \in H, \tag{1d}$$

$$x_{n,j,h} - G_{n,j,h}^{u} = x_{n,j,h}^{+} - x_{n,j,h}^{-} \quad \forall n \in \mathbb{N}, \ \forall h \in H,$$
 (1e)

$$0 \le x_{n,j,h}^+ \perp x_{n,j,h}^- \ge 0 \quad \forall n \in \mathbb{N}, \ \forall h \in \mathbb{H}, \tag{1f}$$

$$G_{n,j,h}^{\mathrm{u}} \le G_{n,j,h} \quad \forall n \in \mathbb{N}, \ \forall h \in H,$$
 (1g)

$$x_{n,j,h}^{+} - \delta_{n,j,h} = x_{n,j,h}^{g} \quad \forall n \in \mathbb{N}, \ \forall h \in H,$$

$$\tag{1h}$$

$$C_{n,j,h} = C_{n,j}^{\text{init}} + \sum_{l=1}^{h} (x_{n,j,l}^{-} - \delta_{n,j,l}) \quad \forall n \in \mathbb{N}, \ \forall h \in \mathbb{H},$$
 (1i)

$$x_{n,j,h}, x_{n,j,h}^+, x_{n,j,h}^-, G_{n,j,h}^u, \delta_{n,j,h}, x_{n,j,h}^g, C_{n,j,h} \ge 0$$

$$\forall n \in N, \ \forall h \in H,$$
(1j)

where $\Psi_{\mathbf{n},\mathbf{j}}^{\mathrm{user}} = \{x_{n,j,h}, x_{n,j,h}^+, x_{n,j,h}^-, G_{n,j,h}^{\mathrm{u}}, \delta_{n,j,h}, x_{n,j,h}^{\mathrm{g}}, C_{n,j,h}\}$. As seen in (1a), end users want to minimise their electricity cost and discomfort caused by load shifting. The prosumers' electricity cost consists of the energy payment at PD prices, $\lambda_{j,h}^{\mathrm{PD}}$, for consumption from the grid, $x_{n,j,h}^{\mathrm{g}}$, and network usage charges, i.e., $\lambda_{j,h}^{\mathrm{ExP}}$ and $\lambda_{j,h}^{\mathrm{ImP}}$, for exported, $x_{n,j,h}^-$, and imported (consumed) electricity, $x_{n,j,h}^+$, respectively. Here, the network usage charges are set by the DNSPs.

The (dis)comfort model is integrated with the time inconsistency and loss aversion properties of behavioural economics as introduced in [25]. In particular, time inconsistency is represented by the fraction in the last term of (1a), which depends on the degree of short-term discounting, κ_n , and the degree of long-term discounting, τ_n . On the other hand, loss aversion is modelled by a quadratic function in (1b) that depends on actual consumption, $x_{n,j,h}$, expected consumption, $\hat{x}_{n,j,h}$, price elasticity, $\beta_{n,j,h}$, and price reference, $\lambda_{\max,j}^{\text{PD}} := \max\{\lambda_{j,h}^{\text{PD}} | h \in H\}$, which is adopted from [25]. In this context, the price elasticity $\beta_{n,j,h}$ indicates the degree to which the consumption of a user varies according to changes in electricity prices, where smaller values denote greater inelasticity. In contrast, the price reference $\lambda_{\max,j}^{\text{PD}}$ acts as a standard for users to assess whether the prices during each interval are elevated or reduced.

Constraint (1c) ensures that the demand response is only provided by load shifting such that in each receding horizon, the sum of actual consumption remains the same as the total expected consumption and the consumption deviation from the previous receding horizons, $\Delta x_{n,j}$. To make the model realistic, unlike existing studies, e.g., [28, 6], we enforce the rebound effect of shiftable loads within the first few hours rather than the whole receding horizon. Therefore, H^{RB} denotes the rebound horizon such that $H^{RB} \subset H$. Constraint (1d) sets the lower, $\underline{x}_{n,j,h}$, and upper, $\overline{x}_{n,j,h}$, bounds of consumption in each interval. Constraint (1e) separates the net demand into exported and imported (consumed) electricity and restricts them from simultaneously having non-zero

values through the complementarity constraint (see [29]) in (1f).

In Australia, renewable energy constitutes a large proportion of the energy mix. This has often led to wholesale prices dropping below zero, sometimes reaching as low as -\$1000/MWh [30]. As a result, the optimal strategy during these intervals is to curtail solar generation. To do this, we consider 'used' solar energy, $G_{n,i,h}^{u}$, in (1e) and constrain it in (1g). Constraint (1h) determines the energy imported from the utility grid, $x_{n,j,h}^{g}$, after deducting the offset by the solar credits, denoted by $\delta_{n,j,h}$. Solar credits are earned when users export excess rooftop solar generation to the grid and can be used later to offset electricity consumption, typically during the evening. The decision to use or conserve these credits is driven by RT price signals, which requires solving an optimisation problem to decide whether to use credits immediately or postpone their use for periods that might incur higher costs. Constraint (1i) tracks the cumulative solar credit over time, $C_{n,j,h}$, where $C_{n,j}^{\text{init}}$ denotes the initial cumulative solar credit in each receding horizon. Due to the sequential solving of the RHO, we have $C_{n,j}^{\text{init}} = C_{n,j-1}^{\star}$ and $\Delta x_{n,j} = \sum_{l=1}^{j} (\hat{x}_{n,l}^{\star} - x_{n,l}^{\star})$ as parameters determined by the previous receding horizons. We define the variables with (\star) as the optimal values committed in previous receding horizons. Finally, we define the signs of the variables in (1j).

2.2. CBS Operation

The solution to the end-user optimisation problem is the changing consumption behaviour over time. As a result, in the CBS optimisation problem, the uncertain parameter is not only the price but also consumption of the end users, as shown in Fig. 2. For each receding horizon j, the optimisation problem for CBS is as follows:

$$\min_{\mathbf{\Psi}_{j}^{\text{CBS}}} O_{j}^{\text{CBS}} = \sum_{h \in H} \left(\lambda_{j,h}^{\text{PD}} \vartheta_{j,h}^{+} + \lambda^{\text{g}} \vartheta_{j,h}^{\text{g}} + \lambda^{\text{ThP}} P_{j,h}^{\text{dc}} \Delta h \right) - \lambda^{\text{peak}} (\Upsilon_{j}^{\text{local}} - \Upsilon_{j}^{\text{user}})$$
(2a)

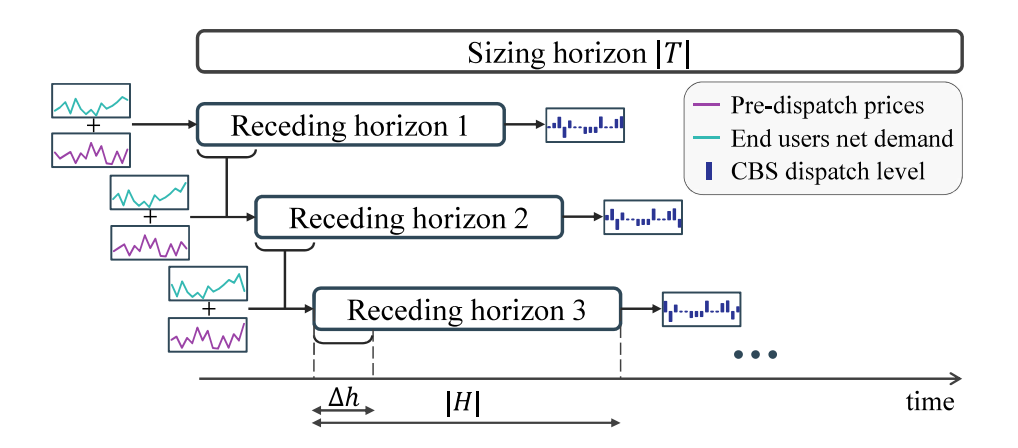


Figure 2: A flowchart showing the CBS RHO framework

s.t.

$$\sum_{n \in N} (x_{n,j,h}^+ - x_{n,j,h}^-) + P_{j,h} \Delta h = \vartheta_{j,h}^+ - \vartheta_{j,h}^- \quad \forall h \in H,$$
 (2b)

$$0 \le \vartheta_{j,h}^+ \perp \vartheta_{j,h}^- \ge 0 \quad \forall h \in H, \tag{2c}$$

$$\Upsilon_j^{\text{local}} \ge \max \left(\vartheta_{j,h}^+, \max_{l \in \{1,2,\dots,j\}} \vartheta_l^{+\star} \right) \quad \forall h \in H,$$
(2d)

$$E_{j,h} = E_j^{\text{init}} + \sum_{l=1}^h \left(P_{j,l}^{\text{ch}} - \frac{1}{\Gamma} P_{j,l}^{\text{dc}} \right) \Delta h \quad \forall h \in H,$$
 (2e)

$$P_{j,h} = P_{j,h}^{\text{ch}} - P_{j,h}^{\text{dc}} \quad \forall h \in H, \tag{2f}$$

$$-\frac{E^{\text{cap}}}{T^{\text{c}}} \le P_{j,h} \le \frac{E^{\text{cap}}}{T^{\text{c}}} \quad \forall h \in H,$$
 (2g)

$$\underline{\text{SoC}} E^{\text{cap}} \le E_{j,h} \le \overline{\text{SoC}} E^{\text{cap}} \quad \forall h \in H, \tag{2h}$$

$$E_j^{\text{init}} = E_{j,h=|H|},\tag{2i}$$

$$P_{j,h}^{\mathrm{ch}} \Delta h - \sum_{n \in N} x_{n,j,h}^{-} \le \vartheta_{j,h}^{\mathrm{g}} \quad \forall h \in H, \tag{2j}$$

$$E_{j,h}, P_{j,h}^{\text{ch}}, P_{j,h}^{\text{dc}}, \vartheta_{j,h}^{+}, \vartheta_{j,h}^{-}, \vartheta_{j,h}^{\text{g}}, \Upsilon_{j}^{\text{local}} \ge 0 \quad \forall h \in H,$$
 (2k)

where $\Psi_{\mathbf{j}}^{\mathrm{CBS}} = \{E_{j,h}, P_{j,h}^{\mathrm{ch}}, P_{j,h}^{\mathrm{ch}}, \partial_{j,h}^{+}, \partial_{j,h}^{-}, \partial_{j,h}^{\mathrm{g}}, \Upsilon_{j}^{\mathrm{local}}\}$. Similar to the end-user problem, the CBS operation is solved sequentially with the initial state-of-charge (SoC), $E_{j}^{\mathrm{init}} = E_{j-1}^{\star}$, passed from the previous horizon as the initial state input, in which the initial value (that is, j=1) is set to zero. The objective of the CBS operator in (2a) is to minimise the net cost. First, it considers wholesale costs, representing payments to the wholesale market for charging the CBS and the electricity consumption by local residential users, $\lambda_{j,h}^{\mathrm{PD}}\vartheta_{j,h}^{+}$. Additionally, it includes the network usage charge, $\lambda^{\mathrm{g}}\vartheta_{j,h}^{\mathrm{g}}$, which applies when electricity is imported from the utility grid for charging the CBS. To avoid excessive cycling of the CBS, a throughput charge, $\lambda^{\mathrm{ThP}}P_{j,h}^{\mathrm{dc}}\Delta h$, is added based on discharging energy. The last term in (2a) represents the revenue from peak demand reduction, which is the difference between the prosumers' peak demand, $\Upsilon_{j}^{\mathrm{user}} = \max\{\sum_{n \in N}(x_{n,j,h}^{+} - x_{n,j,h}^{-}|h \in H)\}$, and the peak demand after considering the CBS operation, $\Upsilon_{j}^{\mathrm{local}}$. Here, DNSPs set the network usage charge, λ^{g} , and the peak demand charge, λ^{peak} .

Constraint (2b) separates the net demand of the whole neighbourhood into imported, $\vartheta_{j,h}^+$, and exported, $\vartheta_{j,h}^-$, electricity. To prevent them from simultaneously taking non-zero values, complementarity constraints (see [29]) are implemented in (2c). We define the peak demand of the local neighbourhood in (2d), which considers both the potential maximum net demand in the lookahead horizon and the observed peak demand in previous receding horizons. Constraint (2e) represents the evolution of the CBS SoC over time, where the charge, $P_{j,h}^{\text{ch}}$, and discharge, $P_{j,h}^{\text{dc}}$, power are defined in (2f). Moreover, in (2e), Γ represents the CBS round-trip efficiency and Δh represents the granularity of the intervals. Constraint (2g) limits the (dis)charging power of CBS with respect to the CBS capacity and battery duration, T^c . Constraint (2h) limits the CBS SoC to the lower, $\underline{\text{SoC}}$, and upper, $\overline{\text{SoC}}$, bounds. To avoid full discharge at the end of each

receding horizon, constraint (2i) sets the ending SoC equal to the initial SoC. Constraint (2j) determines the electricity imported from the utility grid for the CBS charging activity. As mentioned in Section 1, the trial CBS tariffs promote the LUoS. Thus, there is no cost to charge the CBS using excess PV generation of the local neighbourhood. In contrast, the CBS operator must pay a fixed charge, $\lambda^{\rm g}$, when charging from the grid. Finally, (2k) represents the sign of the variables. Note that in the CBS operation, the CBS capacity, $E^{\rm cap}$, is a known parameter.

2.3. Ground Truth Cost Calculation

Since we operate the CBS in (2) with respect to the PD prices, it is necessary to calculate the ground truth cost of the CBS operation by applying the optimised solutions committed from (2) to the RT dispatch (cleared) prices, $\lambda^{\rm RT}$. Additionally, in (2a), we assess the revenue from peak demand reduction for each receding horizon separately. However, in practice, DNSPs typically assess peak demand on a yearly basis. As a result, we calculate the annual ground truth cost as follows:

Total cost =
$$\sum_{j \in J} \left(\lambda_j^{\text{RT}} \vartheta_j^{+\star} + \lambda^{\text{g}} \vartheta_j^{\text{g}\star} + \lambda^{\text{ThP}} P_j^{\text{dc}\star} \Delta h \right) - \lambda^{\text{peak}} (\Upsilon^{\text{local}\star} - \Upsilon^{\text{user}\star}) + \lambda^{\text{bat}} E^{\text{cap}},$$
(3)

where $\Upsilon^{\text{local}\star} = \max\{\vartheta_j^{+\star}|j\in J\}$ and $\Upsilon^{\text{user}\star} = \max\{\sum_{n\in N} (x_{n,j}^{+\star} - x_{n,j}^{-\star})|j\in J\}$. We also include the cost of CBS, $\lambda^{\text{bat}}E^{\text{cap}}$, as part of the total project cost, assuming a battery life expectancy of 10 years, which is in line with the typical manufacturer warranty period. Here, we only consider the net cost of CBS and its operation to provide an accurate comparison among different sizing methods, as introduced in the subsequent section.

3. Battery sizing methods

3.1. Exhaustive Search for (Exact) Battery Sizing

Since the CBS operates under the RHO regime, we cannot obtain the optimal CBS capacity in one single optimisation. Instead, the lowest project cost in (3)

must be determined by examining different values of battery capacity, E^{cap} , for CBS operation in (2). Therefore, in this paper, we iteratively assess all possible CBS capacities with a step of 5 kWh to find the global optimal value.

3.2. One-shot optimisation (W/o RH)

As mentioned in Section 1, a common battery sizing approach is to assume a perfect prediction of uncertain parameters, i.e., electricity prices and prosumers' consumption in this case, and solve a planning problem over the entire sizing horizon. To size the CBS without RHO, we solved a modified version of (2), where instead of looking at all intervals in H, we only considered the first interval in H, i.e., h=1, and sum over $j\in J$ in (2a). Moreover, we remove (2i) because now there is only one ending SoC. We formulate the battery sizing model for the W/o RH method as follows:

$$\min_{\mathbf{\Psi}^{\text{WoRH}}} S^{\text{WoRH}} = \sum_{j \in J} \left(\lambda_j^{\text{RT}} \vartheta_j^+ + \lambda^{\text{g}} \vartheta_j^{\text{g}} + \lambda^{\text{ThP}} P_j^{\text{dc}} \Delta h \right)
- \lambda^{\text{peak}} (\Upsilon^{\text{local}} - \Upsilon^{\text{user}\star}) + \lambda^{\text{bat}} E^{\text{cap}},$$
(4a)

s.t.
$$(2b)-(2c), (2e)-(2h), (2j)$$
 such that $h = 1, \forall j \in J$, (4b)

$$\Upsilon^{\text{local}} \ge \vartheta_j^+ \quad \forall j \in J,$$
(4c)

$$E_{j}, P_{j}^{\mathrm{ch}}, P_{j}^{\mathrm{dc}}, \vartheta_{j}^{+}, \vartheta_{j}^{-}, \vartheta_{j}^{\mathrm{g}}, \Upsilon^{\mathrm{local}}, E^{\mathrm{cap}} \geq 0 \quad \forall j \in J, \tag{4d}$$

where $\Psi^{\text{WoRH}} = \{E_j, P_j^{\text{ch}}, P_j^{\text{dc}}, \vartheta_j^+, \vartheta_j^-, \vartheta_j^{\text{g}}, \Upsilon^{\text{local}}, E^{\text{cap}}\}$. As E^{cap} is a decision variable in this optimisation, we can directly obtain the CBS capacity in a single optimisation process. Note that we have normalised both λ^{peak} and λ^{cap} to align with the length of the receding horizons. In (4a), we use the actual spot prices to represent a scenario with perfect foresight. To evaluate the impact of incorporating uncertainty, as used in [15, 16], we replace the actual spot prices with PD prices. Hence, in this paper, we perform two scenarios for the W/o RH sizing method: one using RT spot prices (W/o RH perfect foresight) and another using 30-minute look-ahead PD prices (W/o RH 0.5-hr PD price).

3.3. Coupled Receding Horizons (Coupled RH)

In [17], the battery sizing and operation are optimised simultaneously considering all receding horizons in one optimisation problem. Therefore, to formulate this problem based on the model in (2), we introduce a new constraint, $E_j^{\text{init}} = E_{j-1,h=1}$, which was originally used to set the initial state parameter on each receding horizon of the CBS operation. We formulate the battery sizing model for the Coupled RH approach as follows:

$$\min_{\mathbf{\Psi}^{\text{CORH}}} S^{\text{CoRH}} = \sum_{\omega \in \Omega} \left[\frac{1}{|H|} \sum_{j \in J_{\omega}} \sum_{h \in H} \left(\lambda_{j,h}^{\text{PD}} \vartheta_{j,h}^{+} + \lambda^{\text{ThP}} P_{j,h}^{\text{dc}} \Delta h + \lambda^{\text{g}} \vartheta_{j,h}^{\text{g}} \right) \right] - \lambda^{\text{peak}} (\Upsilon^{\text{local}} - \Upsilon^{\text{user}}) + \lambda^{\text{bat}} E^{\text{cap}}$$
(5a)

s.t.
$$(2b)$$
– $(2k)$ $\forall j \in J_{\omega}, \forall \omega \in \Omega,$ (5b)

$$E_j^{\text{init}} = E_{j-1,h=1} \quad \forall j \in J_\omega \setminus \{1\}, \ \forall \omega \in \Omega, \tag{5c}$$

$$E_{j,h}, P_{j,h}^{\text{ch}}, P_{j,h}^{\text{dc}}, \vartheta_{j,h}^{+}, \vartheta_{j,h}^{-}, \vartheta_{j,h}^{\text{g}}, \Upsilon^{\text{local}}, E^{\text{cap}} \ge 0$$

$$\forall h \in H, \ \forall j \in J_{\omega}, \ \forall \omega \in \Omega$$
(5d)

where $\Psi^{\text{CoRH}} = \{E_{j,h}, P_{j,h}^{\text{ch}}, P_{j,h}^{\text{dc}}, \vartheta_{j,h}^+, \vartheta_{j,h}^-, \vartheta_{j,h}^{\text{g}}, \Upsilon^{\text{local}}, E^{\text{cap}}\}$. Similar to the W/o RH method, the optimal E^{cap} in the Coupled RH approach can be obtained in a single optimisation process. Because all receding horizons are considered simultaneously, we need to divide the extended battery sizing duration into smaller periods $\omega \in \Omega$, where each period contains $|J_{\omega}|$ receding horizons. This is done to prevent one receding horizon from looking too far ahead into the future. For example, in [17], each receding horizon was 1-hour long with 10-minute granularity, equivalent to |H|=6 in our model. Additionally, their sizing model considered each period to be one full day, i.e., $J_{\omega}=144$. In contrast, our model considers close to one-day look-ahead with 30-minute intervals. As a result, we set each period ω to one week in our study. This timeframe allows the sizing model enough flexibility to establish the RHO without allowing receding

Table 1: Network usage charges and end user elasticity at different time intervals

Interval	$\lambda_{j,h}^{\mathrm{ExP}}$ (¢/kWh)	$\lambda_{j,h}^{\mathrm{ImP}}$ (¢/kWh)	$eta_{n,j,h}$
01:00-05:00	0	3.3095	[-0.2, -0.3]
05:00-10:00	0	3.3095	[-0.3, -0.5]
10:00-14:00	1.8500	3.3095	[-0.3, -0.5]
14:00-20:00	-27.7957	27.7957	[-0.5, -0.7]
20:00-01:00	0	3.3095	[-0.3, -0.5]

Table 2: CBS specifications and simulation parameters

Battery data		Other simulation parameters		
Γ	90%	$\underline{x}_{n,j,h}$	$0.5\hat{x}_{n,j,h}$	
$\underline{SoC},$	0%,100%	$\overline{x}_{n,j,h}$ $\overline{x}_{n,j,h}$	$1.5\hat{x}_{n,j,h}$	
$\overline{\mathrm{SoC}}$				
Δh	0.5 hours	$ H^{ m RB} $	12 (6 hours)	
T^{c}	2 hours	H	32 (16 hours)	
λ^{bat}	$80/\mathrm{kWh\cdot year}$	κ_n	[0.1, 0.5]	
λ^{ThP}	3.2 ¢/kWh	τ_n	0.2	
$\lambda^{ m g}$	1.61 ¢/kWh	$\lambda^{ m peak}$	$0.33 \ \text{kW-year}$	

horizons looking far into the future to interfere with current calculations. Lastly, due to the coupled receding horizons, we need to take the weighted sum of all the receding horizons by dividing over |H| as seen in (5a).

4. Numerical Study

4.1. Simulation Setup

• End user profiles were collected from the Solar Home dataset with 60 solar prosumers and 60 non-solar consumers in New South Wales (NSW), Australia [31]. The dataset contains half-hourly electricity consumption and gross rooftop PV generation in 2012. Due to the increase in rooftop PV capacity

in recent years [32], we uniformly scaled up the PV generation profiles of all prosumers by three times, giving an average rooftop PV capacity of 5.1 kWp.

- Electricity prices and network charges were collected for the NSW region in 2021 [26]. The new network charges for end users, recently tested in that region, and the CBS tariff were collected from the DNSP in NSW [8]. Table 1 shows the end-user network usage charges at different times of the day, where the negative value of λ^{ExP} represents an export reward for rooftop solar PV energy.
- CBS specifications and simulation parameters are summarised in Table 2. At any time of the day, the PD prices in the NEM are available for a minimum of 16 hours ahead [26]. Thus, in our optimisation, the length of one receding horizon is considered to be 16 hours. The price elasticity of electricity demand is relatively low and varies depending on the time of day. To capture this, we randomly generated a price elasticity value, $\beta_{n,j,h}$, for each end user from a uniform distribution based on the time of day. Table 1 shows the time bands and ranges of the distribution.
- Simulation period was divided into in-sample and out-of-sample periods. The in-sample period, comprising the second week of each month (84 days in total) of the selected years, is used to size the CBS capacity. In contrast, the out-of-sample period, which includes the third week of each month (also 84 days), is used to evaluate and confirm the performance of the different sizing methods in Section 3. The code and data used for our simulations can be accessed at [33].

4.2. Simulation Results and Discussions

4.2.1. Predispatch prices and end user consumption

The benefit of battery RHO is its adaptability to changes in forecasts over time. As a result, we require dynamic forecast data to demonstrate this adaptability. Although the (forecast) PD prices can be publicly obtained from the Australian NEM [26], variations in the consumption behaviour of the end user

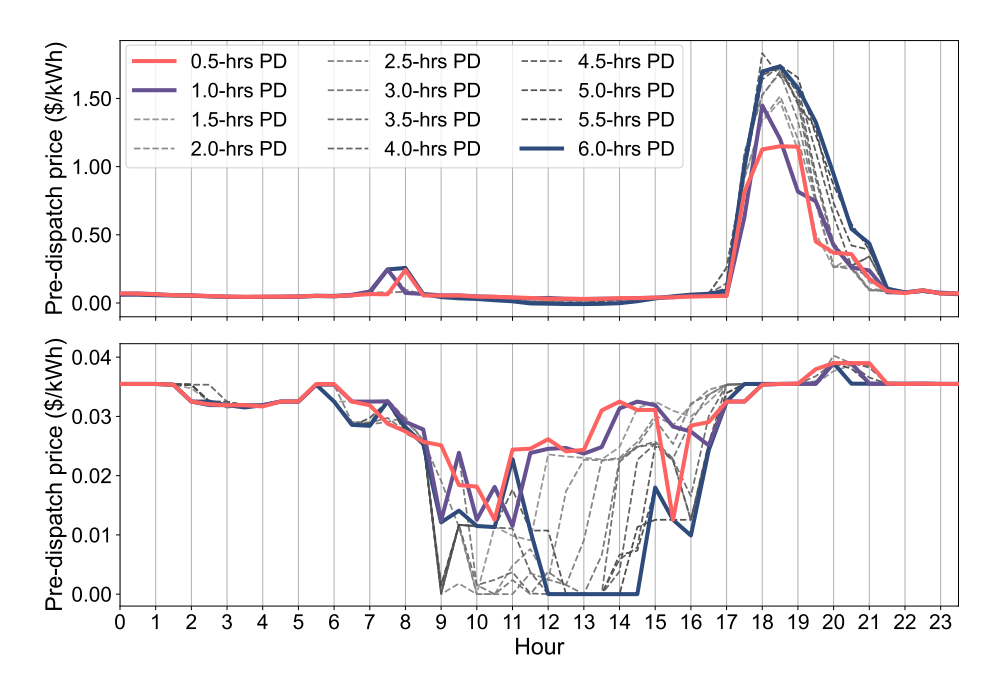


Figure 3: PD prices at different receding horizons. The upper figure depicts average PD prices from the in-sample period, while the lower figure shows the PD prices of a specific day in January

Table 3: Optimal CBS capacity and normalised annual cost with daily average cycle for in-sample and out-of-sample periods

Methods	Capacity	In-sample			Out-of-sample				
	(kWh)	Energy charge	Peak reduction	Total cost	Avg cycle	Energy charge	Peak reduction	Total cost	Avg cycle
Exact 250	250	\$37.8k	-\$13.8k	\$47.5k	1.01	\$53.2k	-\$6.2k	\$70.5k	1.04
	200	\$91.0K	(114.1 kW)	(+0.0%)			(50.8 kW)	(+0.0%)	
W/o RH	320	\$36.3k	-\$13.8k	\$52.1k	0.94	\$51.0k	-\$2.4k	\$78.4k	0.99
perfect foresight	320		(114.1 kW)	(+9.8%)	0.54		(20.0 kW)	(+11.2%)	
W/o RH	468	\$32.9k	-\$13.6k	\$62.3k	0.84	\$45.6k	-\$3.5k	\$85.0k	0.87
0.5-hr PD price	400		(112.3 kW)	(+31.1%)	0.64		(29.2 kW)	(+20.6%)	
Coupled RH	486	\$32.8k	-\$14.0k	\$63.4k	0.83	\$45.4k	-\$3.8k	\$86.2k	0.85
			(115.5 kW)	(+33.4%)			(31.2 kW)	(+22.3%)	

are not readily available from any data source. Instead, we obtain these variations through an analytical model, specifically by solving the optimisation problem in (1). Figures 3 and 4 show changes in PD prices and aggregated expected consumption over time, respectively. To provide context, the values indicated

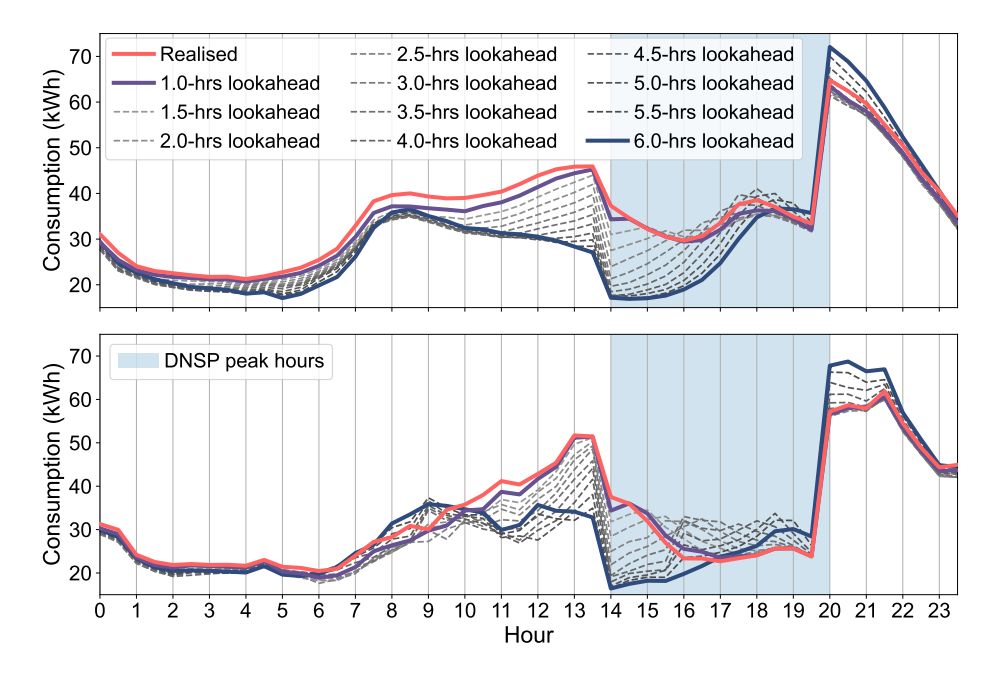


Figure 4: Realised and expected consumption at different receding horizons. The upper figure shows the average consumption from the in-sample period, while the lower figure shows the consumption of the same day as in Fig. 3

by the blue line signify the forecast values obtained using 6 hours of past data; for example, the value at 20:00 was estimated at the receding horizon starting at 14:00. This dynamic behaviour in end-user consumption is achieved by incorporating changing PD prices, coupled with the application of behavioural economic concepts, including loss aversion and time inconsistency, as introduced in [25]. Furthermore, it can be seen that end users perform load shifting with relatively smooth curves, except for a sudden jump at 20:00, immediately after the DNSP peak hours window, which has a network usage charge of more than 27¢/kWh, as shown in Table 1. This behaviour can be observed in real life, as reported by DNSP after one year of trial tariff [34].

4.2.2. Optimal CBS capacities from different sizing methods

Table 3 shows the optimal CBS capacity and normalised annual total cost associated with each method. Note that after determining the optimal CBS

Table 4: Predispatch (PD) prices error analysis for in-sample period

$\sum_{j} (\lambda_{j,h}^{ ext{PD}} - \lambda_{j,h}^{ ext{RT}})$	Mean	Median	SD	Skew	Kurt
0.5-hr PD $(h = 1)$	0.082	0.00	1.167	9.96	144.54
16-hr PD $(h = H)$	0.121	0.00	1.350	8.85	103.04
All intervals	0.132	0.00	1.414	8.68	94.39

capacity using various sizing methods, we run the CBS operation model in (2) and calculate the cost using (3). We also quantify the percentage of financial losses for the W/o RH and Coupled RH methods compared to the *Exact* model, as shown by the percentage values in round brackets. Clearly, the Exact method, which applies RHO with imperfect forecasts during the sizing stage, provides the lowest cost in the in-sample period. This method identifies a globally optimal capacity of 250 kWh using an exhaustive search. The result is then confirmed using the data from the out-of-sample, which also gives the lowest cost among the CBS capacities obtained.

It should be noted that the Exact method resulted in the highest energy charge, which can be attributed to its smaller battery capacity (250 kWh). While this smaller size limits the battery's ability to perform energy arbitrage, the trade-off ultimately delivers the lowest overall cost to the community due to the combination of a lower battery cost and a substantial reduction in the cost of peak demand. This highlights the importance of careful sizing during the planning phase, where achieving optimal cost balance is more critical than simply minimising one component of the cost equation. To further illustrate this trade-off, Fig. 5 shows the variation in individual cost components across a range of CBS capacities for in-sample data. As CBS size increases, peak demand is reduced, contributing to higher peak reduction revenue. However, this benefit gradually saturates, while the energy charges decrease only marginally. As a result, the total cost curve reaches its minimum at 250 kWh and begins to increase beyond this point due to the linear growth of capital cost.

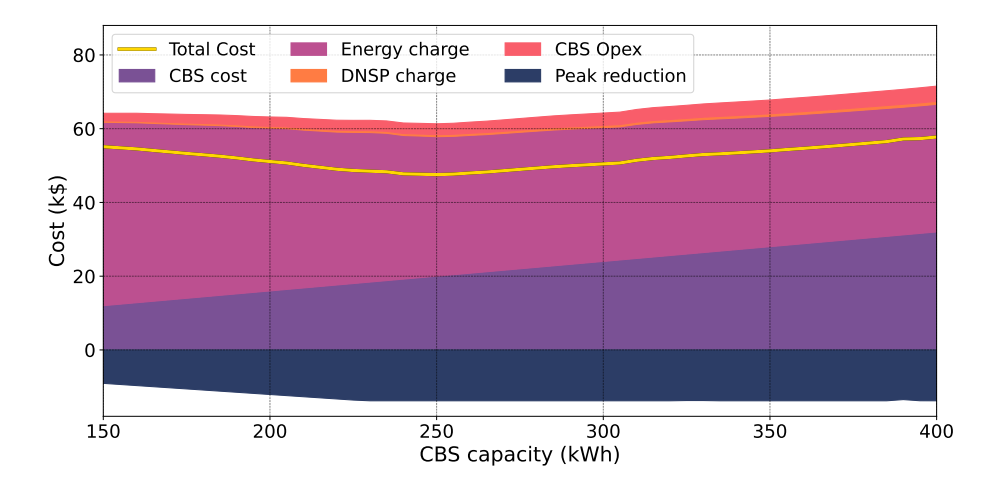


Figure 5: Breakdown of annual cost components across different CBS capacities for the insample data. The total cost (yellow line) reaches its minimum at 250 kWh, indicating the optimal balance point between investment and operational savings.

One key consideration when choosing between methods is computational efficiency. The Exact method requires an exhaustive search, making it computationally expensive and the longest to run. However, this additional effort is justified because it occurs during the planning phase, where the priority is to obtain accurate results rather than speed. Even so, the computational time for the Exact method is reasonable, taking less than a day to complete. On the other hand, one-shot methods such as W/o RH and Coupled RH are significantly faster, with runtimes of only a few minutes, but come at the expense of suboptimal battery size, as shown in the table.

Next, we see that the optimal solution obtained by the Coupled RH method, as proposed in [17], returned the highest CBS capacity, resulting in the highest cost and financial losses. This can be attributed to errors in PD prices, as can be seen in the top panel of Fig. 3 and Table 4. The analysis shows that PD prices are more accurate if they are closer to RT, as shown by the lower mean and standard deviation (SD) in h = 1 than in h = |H| and all intervals combined. Furthermore, high kurtosis indicates that although most errors in PD prices cluster around the distribution mean, there are a few significant outliers. Mostly, these outliers lie on the right-hand side of the distribution

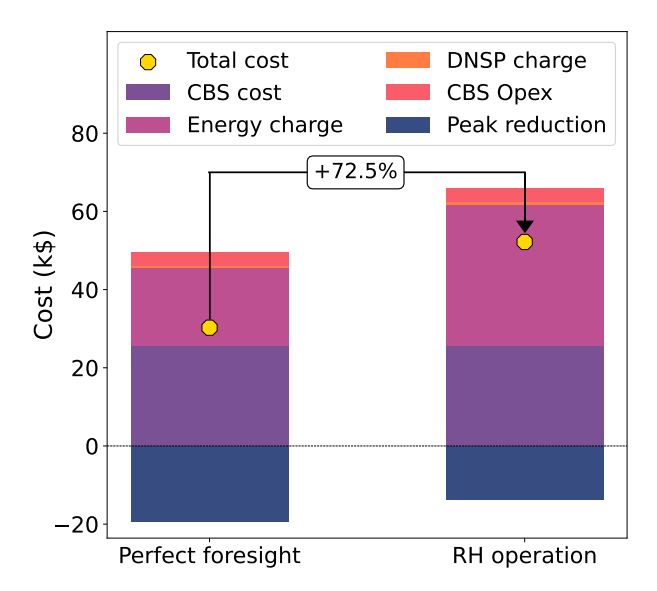


Figure 6: Comparing hypothetical cost from the optimisation under the W/o RH perfect foresight model vs cost from RH operation with imperfect forecasts (realistic operation) model on 320 kWh CBS in the in-sample period

mean, as indicated by the positive skew. Overall, this shows that PD prices generally overestimate true dispatch prices. Consequently, sizing methods that rely heavily on PD prices during the sizing phase, which are the Coupled RH and W/o RH with uncertainty approaches, are prone to oversizing. The W/o RH with uncertainty method, based on [15, 16], uses only the 0.5-hour-ahead PD prices as input for a one-shot optimisation over the entire sizing horizon. While this introduces some level of forecast uncertainty, the method does not dynamically update these forecasts at each interval as would occur in a real-time RHO framework. As a result, it fails to reflect the evolving nature of operational conditions and the continuous adjustment of forecasts that are fundamental to realistic battery operation. Similarly, the Coupled RH method, although it includes a RHO structure, uses PD prices generated for future intervals that would not be available in a real-time setting. This assumption allows future forecast errors to influence current decisions, which deviates from how RHO is implemented in practice.

Although the W/o RH method with perfect foresight, as adopted in [11, 12],

produces the storage size closest to the global optimal value, it still oversizes the CBS capacity, leading to financial losses of approximately 9.8% and 11.2% in the in-sample and out-of-sample periods, respectively. This behaviour can be explained by the under-utilised CBS capacity in actual operation. Figure 6 compares the total costs of CBS capacity of 320 kWh between perfect foresight and RHO with imperfect forecast scenarios. Since the CBS capacity of 320 kWh is the optimal solution from the W/o RH method with perfect foresight, its cost breakdown can be obtained directly from the optimised solutions in (4). As a result, it represents the minimum cost that the 320 kWh CBS can achieve. In contrast, the cost breakdown for the RHO with imperfect forecasts is obtained by running the CBS operation model in (2) for the 320 kWh CBS. It can be seen that the total cost difference lies mainly in the energy charge and revenue from peak demand reduction. While the energy charge depends heavily on the PD prices, the revenue from peak demand reduction depends greatly on the end-user (peak) consumption forecast.

The under-utilisation of CBS in the actual operation is also reflected in the daily average CBS cycle, as shown in Table 3. Due to the imperfect forecast of price and consumption variations, CBS may overlook opportunities for energy arbitrage. This can lead to reduced daily charging and discharging activities, particularly when dealing with higher CBS capacities. In both in-sample and out-of-sample studies, the battery size obtained from the Exact method experiences almost one cycle per day, which is the default warranty term across battery manufacturers.

4.2.3. Impact of CBS capacity on peak demand reduction

Contrary to the prevailing view, a higher CBS capacity does not guarantee a greater reduction in peak demand. It can be observed in the out-of-sample period in Table 3 that the lowest CBS capacity (250 kWh) results in the highest peak demand reduction (50.8 kW). As previously explained, the ability to reduce peak demand depends greatly on the end-user (peak) consumption forecast. It is shown in Fig. 4 that predicted consumption (e.g., the blue line)

could be higher than actual (realised) consumption. Consequently, the CBS optimisation model miscalculates the actual peak demand and charges the CBS in earlier intervals, causing a new peak for the local neighbourhood. The higher the maximum CBS power, the higher the new peak, causing a lower reduction in peak demand. This issue has also been observed in real life in which a 1.1MW/2.15MWh battery in the distribution network caused a higher peak demand when performing energy arbitrage [35]. Thus, it is crucial to ensure that CBS operates without detrimentally impacting distribution networks and remains a vital area for research.

5. Conclusion

In this paper, we shed light on the impact of simplified models in state-of-the-art battery sizing studies, namely the W/o RH and Coupled RH approaches. To accurately quantify the financial losses from these simplifications, we developed a mathematical framework for a CBS-related business model using trial tariffs from an Australian DNSP. We showed that the Coupled RH technique produced the least accurate results with significantly higher cost and CBS capacity than the Exact model, which considers the practical battery RHO. Although the W/o RH method, under perfect foresight, resulted in oversized battery capacity, the resulting financial losses were less significant. Lastly, we highlight a potential scenario in which CBS can negatively affect distribution networks by introducing new peak demand due to CBS arbitrage.

Key findings of this study:

- The RHO approach with imperfect forecasts (*Exact* model) results in the most financially efficient CBS capacity.
- The Coupled RH method leads to significant oversizing and cost overestimation due to unrealistic forecast assumptions.
- The W/o RH method, although based on perfect foresight, performs moderately well but still introduces bias due to oversizing.

• CBS arbitrage, if not carefully managed, can shift demand and create new peak load issues in the distribution network.

In our future work, we aim to extend this analysis to include other market services provided by CBS and explore profitable business models under evolving tariff structures.

References

- [1] Synergy, Alkimos beach energy storage trial final report (2021).
 URL https://arena.gov.au/knowledge-bank/alkimos-beach-energy-storage-trial-final-report/
- [2] Yarra, Yarra community battery project (2022).
 URL https://www.yef.org.au/community-batteries/yarra-community-battery-trial/
- [3] Ausgrid, Community batteries (2022).

 URL https://www.ausgrid.com.au/In-your-community/Community-B
 atteries
- [4] C. P. Mediwaththe, M. Shaw, S. Halgamuge, D. B. Smith, P. Scott, An incentive-compatible energy trading framework for neighborhood area networks with shared energy storage, IEEE Transactions on Sustainable Energy 11 (1) (2020) 467–476. doi:10.1109/TSTE.2019.2895387.
- [5] H. Ransan-Cooper, B. C. P. Sturmberg, M. E. Shaw, L. Blackhall, Applying responsible algorithm design to neighbourhood-scale batteries in australia, Nature Energy 6 (8) (2021) 815–823. doi:10.1038/s41560-021-00868-9. URL https://doi.org/10.1038/s41560-021-00868-9
- [6] N. T. Dinh, S. A. Pourmousavi, S. Karimi-Arpanahi, Y. P. S. Kumar, M. Guo, D. Abbott, J. A. R. Liisberg, Optimal sizing and scheduling of community battery storage within a local market, in: Proceedings of the

Thirteenth ACM International Conference on Future Energy Systems, e-Energy '22, Association for Computing Machinery, New York, NY, USA, 2022, p. 34–46. doi:10.1145/3538637.3538837.
URL https://doi.org/10.1145/3538637.3538837

- [7] A. E. Regulator, Tariff trials (2022).
 URL https://www.aer.gov.au/networks-pipelines/network-tariff-reform/tariff-trials
- [8] Ausgrid, Trial tariffs network price list 2022-2023 (2022).
 URL https://cdn.ausgrid.com.au/-/media/Documents/Regulation/Pricing/PList/Ausgrids-Trial-Tariffs-Network-Price-List-2022-23.pdf
- [9] Ausgrid, Ausgrid sub-threshold tariffs 2022-23 (2022).
 URL https://www.aer.gov.au/system/files/Ausgrid%20-%20Tariff
 %20trial%20notification%20-%202022-23_0.pdf
- [10] R. Khezri, A. Mahmoudi, H. Aki, Optimal planning of solar photovoltaic and battery storage systems for grid-connected residential sector: Review, challenges and new perspectives, Renewable and Sustainable Energy Reviews 153 (2022) 111763. doi:https://doi.org/10.1016/j.rser.2021. 111763.

URL https://www.sciencedirect.com/science/article/pii/S13640 32121010339

- [11] D. Huo, M. Santos, I. Sarantakos, M. Resch, N. Wade, D. Greenwood, A reliability-aware chance-constrained battery sizing method for island microgrid, Energy 251 (2022) 123978. doi:https://doi.org/10.1016/j.en ergy.2022.123978.
 - URL https://www.sciencedirect.com/science/article/pii/S03605
 44222008817
- [12] R. Khezri, A. Mahmoudi, M. H. Haque, A demand side management approach for optimal sizing of standalone renewable-battery systems, IEEE

- Transactions on Sustainable Energy 12 (4) (2021) 2184–2194. doi: 10.1109/TSTE.2021.3084245.
- [13] T. Weckesser, D. F. Dominković, E. M. Blomgren, A. Schledorn, H. Madsen, Renewable energy communities: Optimal sizing and distribution grid impact of photo-voltaics and battery storage, Applied Energy 301 (2021) 117408. doi:https://doi.org/10.1016/j.apenergy.2021.117408. URL https://www.sciencedirect.com/science/article/pii/S03062 61921008059
- [14] Aurora Energy Research, What goes wrong when modelling & forecasting grid-scale battery investment cases?, https://auroraer.com/sector/flexible-energy-storage/what-goes-wrong-when-modelling-forecasting-grid-scale-battery-investment-cases/, accessed: 2025-04-02 (2023).
- [15] Y. Zhang, A. Lundblad, P. E. Campana, F. Benavente, J. Yan, Battery sizing and rule-based operation of grid-connected photovoltaic-battery system: A case study in sweden, Energy Conversion and Management 133 (2017) 249-263. doi:10.1016/j.enconman.2016.11.060.
 URL https://www.sciencedirect.com/science/article/pii/S01968 9041631069X
- [16] I. Alsaidan, A. Khodaei, W. Gao, A comprehensive battery energy storage optimal sizing model for microgrid applications, IEEE Transactions on Power Systems 33 (4) (2018) 3968–3980. doi:10.1109/TPWRS.2017.276 9639.
- [17] K. Baker, G. Hug, X. Li, Energy storage sizing taking into account forecast uncertainties and receding horizon operation, IEEE Transactions on Sustainable Energy 8 (1) (2017) 331–340. doi:10.1109/TSTE.2016.2599074.
- [18] S. Taheri, V. Kekatos, S. Veeramachaneni, Energy storage sizing in presence of uncertainty, in: 2019 IEEE Power & Energy Society General Meeting (PESGM), 2019, pp. 1–5. doi:10.1109/PESGM40551.2019.8973568.

- [19] I. N. Moghaddam, B. Chowdhury, M. Doostan, Optimal sizing and operation of battery energy storage systems connected to wind farms participating in electricity markets, IEEE Transactions on Sustainable Energy 10 (3) (2019) 1184–1193. doi:10.1109/TSTE.2018.2863272.
- [20] S. Karimi-Arpanahi, A. P. Kani, N. Mahdavi, Battery scheduling optimisation in energy and ancillary services markets: Quantifying unrealised revenue in the australian nem, in: Proceedings of the 15th ACM International Conference on Future and Sustainable Energy Systems, e-Energy '24, Association for Computing Machinery, New York, NY, USA, 2024, p. 226–236. doi:10.1145/3632775.3661960.

URL https://doi.org/10.1145/3632775.3661960

- [21] J. M. Reniers, G. Mulder, S. Ober-Blöbaum, D. A. Howey, Improving optimal control of grid-connected lithium-ion batteries through more accurate battery and degradation modelling, Journal of Power Sources 379 (2018) 91-102. doi:10.1016/j.jpowsour.2018.01.004. URL https://www.sciencedirect.com/science/article/pii/S03787 75318300041
- [22] E. Balogun, E. Buechler, S. Bhela, S. Onori, R. Rajagopal, Ev-ecosim: A grid-aware co-simulation platform for the design and optimization of electric vehicle charging infrastructure, IEEE Transactions on Smart Grid 15 (3) (2024) 3114–3125. doi:10.1109/TSG.2023.3339374.
- [23] Amber, Amber electric (2022).

 URL https://www.amber.com.au/
- [24] T. Conversation, Smart meters and dynamic pricing can help consumers use electricity when it's less costly, saving money and reducing pollution (2022).
 - URL https://theconversation.com/smart-meters-and-dynamic-pricing-can-help-consumers-use-electricity-when-its-less-costly-saving-money-and-reducing-pollution-190217

- [25] N. T. Dinh, S. Karimi-Arpanahi, R. Yuan, S. A. Pourmousavi, M. Guo, J. A. R. Liisberg, J. Lemos-Vinasco, Modeling irrational behavior of residential end users using non-stationary gaussian processes, IEEE Transactions on Smart Grid 15 (5) (2024) 4636–4648. doi:10.1109/TSG.2024.3 382771.
- [26] AEMO, Aemo market portals (2022).

 URL https://aemo.com.au/
- [27] N. E. Market, National electricity market (2023).

 URL https://www.dcceew.gov.au/energy/markets/national-electricity-market
- [28] L. Werner, A. Wierman, S. H. Low, Pricing flexibility of shiftable demand in electricity markets, in: Proceedings of the Twelfth ACM International Conference on Future Energy Systems, e-Energy '21, Association for Computing Machinery, New York, NY, USA, 2021, p. 1–14. doi:10.1145/3447555.3464847.
 URL https://doi.org/10.1145/3447555.3464847
- [29] S. A. Gabriel, A. J. Conejo, J. D. Fuller, B. F. Hobbs, C. Ruiz, Complementarity Modeling in Energy Markets, Vol. 180 of International Series in Operations Research & Management Science, Springer, New York, NY, 2013. doi:10.1007/978-1-4419-6123-5.
 - URL https://link.springer.com/book/10.1007/978-1-4419-6123-5
- [30] AEMO, The national electricity market (2023).

 URL https://aemo.com.au/-/media/files/electricity/nem/nation
 al-electricity-market-fact-sheet.pdf
- [31] Ausgrid, Solar home electricity data (2012).

 URL https://www.ausgrid.com.au/Industry/Our-Research/Data-t
 o-share/Solar-home-electricity-data

- [32] A. E. Council, Solar report quarter 3, 2021, Tech. rep. (2021).

 URL https://www.energycouncil.com.au/media/5zylveyr/australi
 an-energy-council-solar-report_q3-2021.pdf
- [33] N. T. Dinh, Github project (2023).

 URL https://github.com/nam-dinh-codes/community-battery-siz
 ing-study
- [34] Ausgrid, 2023-24 sub-threshold tariff notification (2023).
 URL https://www.aer.gov.au/system/files/Ausgrid%20-%20Tariff
 %20trial%20notification%20-%202023-24.pdf
- [35] T. U. of Queensland, The business case for behind-the-meter energy storage (2020).

URL https://sustainability.uq.edu.au/files/11868/EPBQtyRptq1
2020.pdf